Disc formation and the origin of clumpy galaxies at high redshift

Agertz, O ; Teyssier, R ; Moore, B

Abstract: Observations of high-redshift galaxies have revealed a multitude of large clumpy rapidly star-forming galaxies. Their formation scenario and their link to present-day spirals are still unknown. In this Letter, we perform adaptive mesh refinement simulations of disc formation in a cosmological context that are unrivalled in terms of mass and spatial resolution. We find that the so-called 'chain-galaxies' and 'clump-clusters' are a natural outcome of early epochs of enhanced gas accretion from cold dense streams as well as tidally and ram-pressured stripped material from minor mergers and satellites. Through interaction with the hot halo gas, this freshly accreted cold gas settles into a large disc-like system, not necessarily aligned to an older stellar component, that undergoes fragmentation and subsequent star formation, forming large clumps in the mass range 107–109 M . Galaxy formation is a complex process at this important epoch when most of the central baryons are being acquired through a range of different mechanisms – we highlight that a rapid mass loading epoch is required to fuel the fragmentation taking place in the massive arms in the outskirts of extended discs, an accretion mode that occurs naturally in the hierarchical assembly process at early epochs.

DOI: https://doi.org/10.1111/j.1745-3933.2009.00685.x

Originally published at:
Agertz, O; Teyssier, R; Moore, B (2009). Disc formation and the origin of clumpy galaxies at high redshift. Monthly Notices of the Royal Astronomical Society, 397(1):L64-L68.
DOI: https://doi.org/10.1111/j.1745-3933.2009.00685.x

Mon. Not. R. Astron. Soc. **000**, 000–000 (0000) Printed 18 August 2009 (MN LaTeX style file v2.2)

Disk formation and the origin of clumpy galaxies at high redshift

Oscar Agertz[1⋆], Romain Teyssier[1,2], Ben Moore[1]

[1] *Institute for Theoretical Physics, University of Zürich, CH-8057 Zürich, Switzerland*
[2] *CEA Saclay, DSM/IRFU/SAp, Batiment 709, 91191 Gif-sur-Yvette Cedex, France*

18 August 2009

ABSTRACT

Observations of high redshift galaxies have revealed a multitude of large clumpy rapidly star-forming galaxies. Their formation scenario and their link to present day spirals is still unknown. In this *Letter* we perform AMR simulations of disk formation in a cosmological context that are unrivaled in terms of mass and spatial resolution. We find that the so called "chain-galaxies" and "clump-clusters" are a natural outcome of early epochs of enhanced gas accretion from cold dense streams as well as tidally and ram-pressured stripped material from minor mergers and satellites. Through interaction with the hot halo gas, this freshly accreted cold gas settles into a large disk-like system, not necessarily aligned to an older stellar component, that undergoes fragmentation and subsequent star formation, forming large clumps in the mass range $10^7 - 10^9\,M_\odot$. Galaxy formation is a complex process at this important epoch when most of the central baryons are being acquired through a range of different mechanisms - we highlight that a rapid mass loading epoch is required to fuel the fragmentation taking place in the massive arms in the outskirts of extended disks, an accretion mode that occurs naturally in the hierarchical assembly process at early epochs.

Key words: accretion - cold flows - galaxies:evolution - galaxies:formation - galaxies:haloes

1 INTRODUCTION

The morphology and star formation properties of high redshift galaxies are very different from present day quiescent spirals and ellipticals. Large clumpy irregular disks with kpc-sized star forming clumps as massive as $M_{\rm cl} \sim 10^7 - 10^9\,M_\odot$ are observed in the Hubble Ultra Deep Field (e.g. Elmegreen et al. 2007, 2009), a population that is very rare today. "Chain galaxies", first identified by Cowie et al. (1995), are believed to be high-redshift disky galaxies seen edge-on, while "clump cluster" galaxies are their face on counterparts (Dalcanton & Shectman 1996; Elmegreen et al. 2004). In optically selected samples, high redshift galaxies show very high star formation rates up to $100-200\,M_\odot{\rm yr}^{-1}$ (Daddi et al. 2004) and in recent spectroscopic observations they appear to be extended, though perturbed, rotating disks (Genzel 2006; Förster Schreiber 2006; Genzel 2008). The origin of these galaxies and how they connect and possibly evolve into present day spirals is still unknown. Although it is possible that major mergers can give rise to large, rotating disks (Robertson & Bullock 2008) and trigger the formation of massive clumps, from globular clusters (Bournaud et al. 2008) to tidal dwarf galaxies (Elmegreen et al. 1993; Barnes & Hernquist 1992), they are not frequent enough, and are more likely to be the origin of the rare, extremely high star forming, sub-millimeter galaxies (Zheng et al. 2004; Jogee 2008; Wall et al. 2008; Tacconi 2008).

Observational evidence (Elmegreen & Elmegreen 2006; Bournaud et al. 2008; Shapiro 2008) suggests that clumps form in gas rich spiral disks rather than during on-going mergers, although the latter scenario can not be completely ruled out (Taniguchi & Shioya 2001; Overzier et al. 2008). Recent work by Bournaud et al. (2007) (hereafter B07) and Elmegreen et al. (2008) has demonstrated that internal disk fragmentation can effectively reproduce many of the observables of chain and clump clusters galaxies and that these different clumpy systems can have the same origin but observed at different inclinations. However, the models of B07 still rely on idealized, pre-existing very massive and asymmetric gas disks, in order to reproduce the massive clumps and their extended positions.

How galaxies acquire their baryons is an open question. The classic picture of galaxy formation within the cold dark matter (CDM) scenario assumes that the accreted

⋆ agertz@physik.unizh.ch

gas is shock heated to the virial temperature, cools radiatively and rains down to form an inner star-forming rotating disk. Recent theoretical studies (Birnboim & Dekel 2003; Kereš et al. 2005; Dekel & Birnboim 2006a; Ocvirk et al. 2008; Dekel et al. 2008; Keres et al. 2008; Brooks et al. 2008) have demonstrated that accretion of fresh gas via cold infall can in fact be the dominant process for gas accretion for halo masses $M \lesssim 10^{11.6}\,M_\odot$. In these halos, the cooling time for gas of temperature $T \sim 10^4$ K is shorter than the timescale of gas compression and shocks are unable to develop. Cold accretion persists in halos above this mass at $z \gtrsim 2$ whilst the classical hot mode of gas accretion dominates at lower z. Because of insufficient spatial resolution, these studies could not follow the evolution of the accreting gas and how the cold streams connect to the central galaxies. The purpose of this *Letter* is to look in detail at the gas accretion and disk formation process using the highest resolution numerical study of galaxy formation ever performed. In particular we will make a connection to the observed properties of the clumpy high redshift galaxies.

2 NUMERICAL SIMULATION

We use the AMR code `RAMSES` (Teyssier 2002) to simulate the formation of a massive disk galaxy in a cosmological context including dark matter, gas and stars. The gas dynamics is calculated using a second-order unsplit Godunov method, while collisionless particles (including stars) are evolved using the Particle-Mesh technique. The modelling includes realistic recipes for star formation (Rasera & Teyssier 2006), supernova feedback and enrichment (Dubois & Teyssier 2008). Metals are advected as a passive scalar and are incorporated self-consistently in the cooling and heating routine, as in Agertz et al. (2009), and we adopt an initial metallicity of $Z = 10^{-3} Z_\odot$ in the high-resolution region. This also serves as a flag for allowed regions of refinement. The refinement strategy is based on a Quasi-Lagrangian approach, so that the number of particles per cell remains roughly constant, avoiding discreteness effects (e.g. Romeo et al. 2008). The computational domain is a 40 Mpc cube containing nested AMR grids of particles and gas cells down to a Lagrangian region containing dark matter particles of mass $M_{\rm p} = 2.2 \times 10^5\,M_\odot$. The effective resolution of our initial grid is therefore 2048^3. We then refine this base grid according to our refinement strategy, so that the maximum resolution is $\Delta x \sim 40$ pc in *physical units* at all times.

For our initial conditions we take the Via-Lactea II simulation (Diemand et al. 2008) which forms a Milky Way sized dark matter halo that accretes most of its mass ($M_{\rm vir} = 2 \times 10^{12}\,M_\odot$) by a redshift $z = 2$. We evolved the entire simulation to $z = 0$ at a coarser resolution, here we report on the high redshift evolution to $z = 2$ at which point it hosts a disk that is massive enough to be compared to the observations in e.g. Bournaud et al. (2008) and Genzel (2006). We use standard galaxy formation ingredients, with a star formation efficiency of 2% (as defined in Rasera & Teyssier (2006)), a star formation density threshold $n_H = 4\,{\rm cm}^{-3}$ and a supernovae mass loading factor $f_w = 10$ (as defined in Dubois & Teyssier (2008)). In order to prevent artificial fragmentation, we use a pressure floor $P \simeq 3G\Delta x^2 \rho^2$, so that we satisfy the Truelove et al. (1997) criterion at any time.

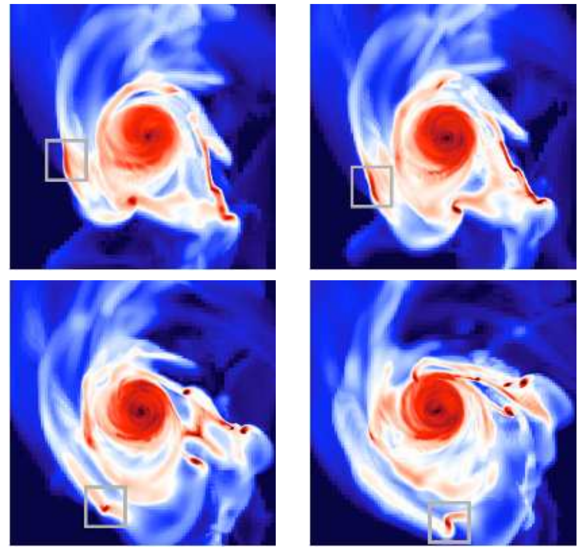

Figure 2. A time sequence spanning 40 Myr of the projected gas density at $z \sim 3$ in a 18×18 kpc^2 region. The grey box show the formation of a $\sim 10^8\,M_\odot$ clump, illustrating the fragmentation process discussed in the text.

3 RESULTS

Fig. 1 shows a large scale view of the galactic disk at $z \sim 3$. At this time the dark matter halo has reached a mass of $M_{\rm vir} \sim 3.5 \times 10^{11}\,M_\odot$, putting it in a regime where both cold flows and stable shocks can exist (Birnboim & Dekel 2003; Dekel & Birnboim 2006a; Ocvirk et al. 2008). This striking image ties together many aspects present in modern theories of galaxy formation and highlights new complexities. Cold streams of gas originating in narrow dark matter filaments, effectively penetrate the halo and transport cold metal-poor gas right down to the proto-galactic disk to fuel the star forming region. A comparable amount of metal enriched material reaches the disk in a process that has previously been unresolved - material that is hydrodynamically stripped from accreting satellites, themselves small disky systems, through the interaction with the hot halo and frequent crossings of the cold streams.

The cold gas streams into the halo on a highly radial trajectory, eventually forming more orderly rotational motion in an extended disk through two mechanisms: A cold stream can gravitationally swing past the halo center and subsequently collide with a cold stream inflowing from an opposite direction; As the cold stream enters the inner halo it also feels a high confining pressure from the hot halo which has a significant rotational component within ~ 40 kpc. Shocks from these collisional processes are quickly dissipated since the cooling times are very short resulting in a denser configuration for the cold gas. As the infalling stripped material and streams lose their radial energy through these interactions, it connects to the inner disk as extended dense spiraling arms that progressively slow down to match the highly ordered inner disk rotation. Fig. 2 shows a time se-

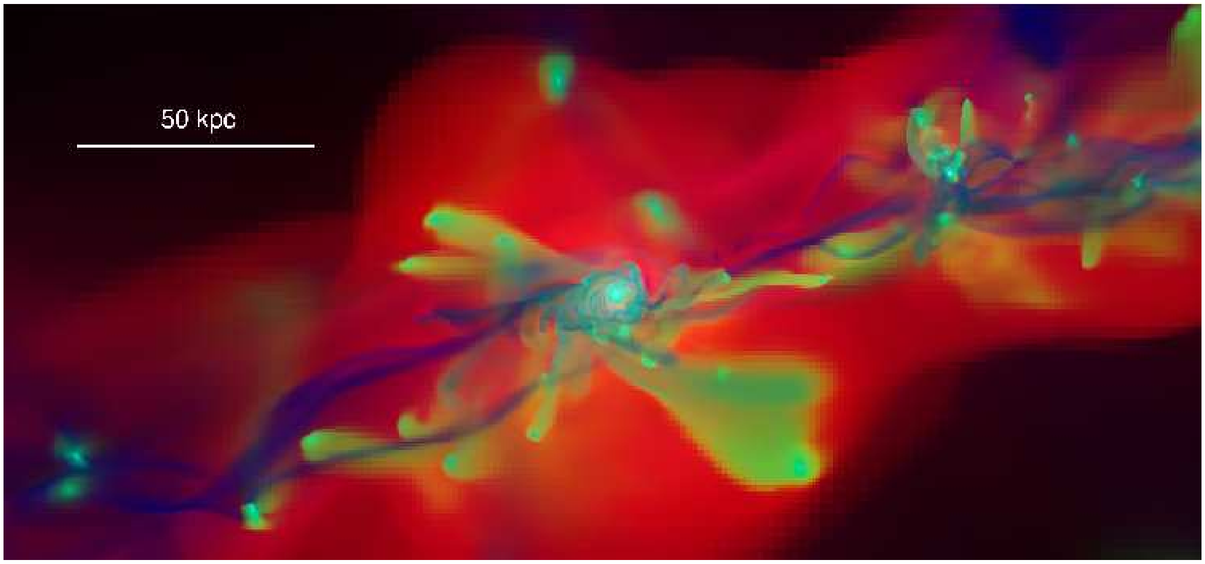

Figure 1. An *RGB*-image of the gas showing the disk and accretion region at $z \sim 3$. The image is constructed using R=temperature, G=metals and B=density. We can clearly distinguish the cold pristine gas streams in blue connecting directly onto the edge of the disk, the shock heated gas in red surrounding the disk and metal rich gas in green being stripped from smaller galaxies interacting with the halo and streams of gas. The disk and the interacting satellites stand out since they are cold, dense and metal rich. The distance measure is in physical units.

quence of the complicated and asymmetric gas flows around the gas disk at $z \sim 3$. The figure reveals that many of the large scale spiral arms at large radii are not waves, but material arms that can survive for an orbital time and that these arms are gravitationally unstable and can fragment into clumps. The grey square in the figure shows the formation of a $\sim 10^8\,\mathcal{M}_\odot$ clump within one of these arms that originated from the cold streams. Gravitational instability has been used by Elmegreen et al. (1993) (hereafter E93) to explain the formation of massive clumps, as large as dwarf galaxies, in the tidal tails of merging galaxies. The typical mass of objects that form within the arms is

$$M_{\rm J} \simeq \frac{\sigma^4}{G^2\Sigma} \tag{1}$$

where Σ is the surface density of gas within the arm and σ is the gas velocity dispersion. Using the small region highlighted by the grey square in Fig. 2, we have computed $\Sigma \simeq 60\,M_\odot$ pc^{-2} and $\sigma \simeq 20$ km s^{-1}, giving $M_{\rm J} \simeq 2 \times 10^8\,M_\odot$. The instability is triggered due to the high surface mass density of the rapidly growing outer disk combined with the compression and shocks that occur from the complex interactions discussed above. The internal dispersion velocity due to turbulent motions within the cold streams is roughly equal to the divergent motions across the curved gas filament. The typical velocity dispersion across the $\lambda \sim 1$ kpc stream will be of the order

$$\sigma \simeq \frac{\lambda}{\mathcal{R}_{\rm c}} v_{\rm orb} \simeq 20\ {\rm km\,s^{-1}} \tag{2}$$

where the orbital velocity $v_{\rm orb}$ is of the order of 200 km s^{-1} and the curvature radius $\mathcal{R}_{\rm c}$ of the streams equals the radius of the extended disk. The fragmentation within the infalling cold streams is similar to that occurring in the tidal tails resulting from major mergers (E93) - the large velocity dispersions giving rise to large clump masses. As the interaction region grows in mass and develops a more symmetric disk-like morphology we also observe massive clump formation in fragmenting spiral waves at intermediate radii. We note that this mass-accretion induced fragmentation is analogous to modern theories of giant gas planet formation at large radii in proto-stellar disks (Boley, private communication).

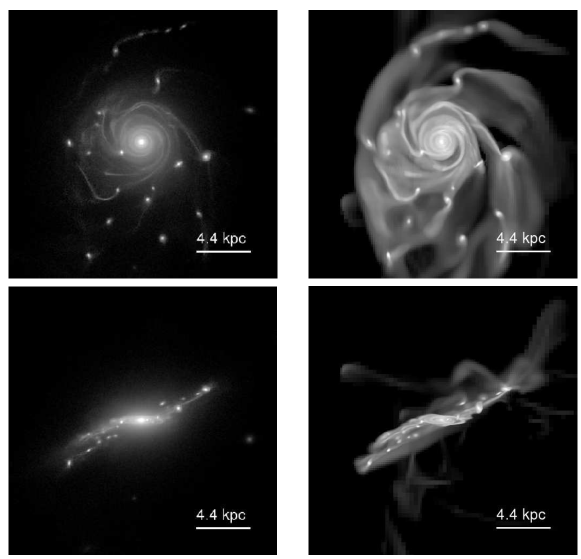

Figure 3. Density projection of the stars (*left*) and gas (*right*) at $z \sim 2.7$ illustrating the fragmentation process and the formation of large clumps of mass $\sim 10^7 - 10^9\,M_\odot$.

The resulting galaxy is shown in Fig. 3 at $z \sim 2.7$, after many large clumps have formed through the above mechanisms. We detect 12 clumps with masses between $M_{\rm cl} = 5 \times 10^7$ and $10^9 M_\odot$, only two of these contained dark matter and were infalling satellites. In the interaction region between the disk and the cold streams, the typical arm surface density and velocity dispersion can both be estimated using mass average quantities within cylindrical shells. At ($r \sim 8$ kpc) we measure $\langle\Sigma\rangle \simeq 20\ \mathrm{M}_\odot\ \mathrm{pc}^{-2}$ and $\langle\sigma\rangle \simeq 30\ \mathrm{km\ s}^{-1}$, giving rise to clump masses as large as $M_\mathrm{J} \simeq 10^9\,M_\odot$. These clumps are located in the interaction region between the disk and the cold streams. In our case this region is not aligned with the initial galactic disk, giving rise to a misalignment of the clumps with respect to the inner galactic disk (see edge-on images in Fig. 3). Although we believe that this misalignment is not typical, it is an elegant explanation for the formation of "bent" chains, such as the one reported in Bournaud et al. (2008). Indeed, Elmegreen & Elmegreen (2006) report that the typical chain galaxy has clumps mostly aligned in the midplane, while in some cases, clumps are seen above and below the midplane (outer and inner disk misaligned). In our case, the misalignment is due to a third cold stream that is perpendicular to the main filament seen in Fig. 1. In a similar scenario, this process has also been invoked to explain the formation of large polar rings (Macciò et al. 2006).

The simulated galaxy is sharing many properties with observed chain and clump cluster galaxies (Elmegreen et al. 2007). Viewed edge-on, the misaligned disk morphology is clearly seen and the overall structure resembles a large chain-galaxy. Viewed face on the spiral-like structure has a similar morphology as clump clusters or clumpy spirals. Elmegreen & Elmegreen (2005) report that UDF clumpy galaxies at $z \sim 1-2$ have a stellar mass $\simeq 6 \times 10^{10}\,M_\odot$ and a radius ~ 10 kpc, in striking agreement with our simulated galaxy. Not only does our scenario reproduce the observed clumpy morphology and global rotation of these systems but we also find a realistic metallicity gradient and star formation rate of 20 $M_\odot\mathrm{yr}^{-1}$. The inner disk has on average solar metallicity, while that in the clump forming region is only $\sim 1/10\,Z_\odot$, due to the accretion of pristine gas in the cold streams mixing with stripped satellite gas. This has the important observational consequence that these massive clumps might be devoid of dust, making them easier to detect.

Cold streams are believed to be the dominant mode of accretion for high-redshift galaxies (Kereš et al. 2005; Dekel & Birnboim 2006b,a; Ocvirk et al. 2008; Dekel et al. 2008). To illustrate this point, we have plotted the mass accretion rate in different gas phases measured around our simulated galaxy at $z = 5, 3$ and 2 in Fig. 4. We define the phases as cold diffuse ($T < 2\times10^5$ K, $n < 0.05\,\mathrm{cm}^{-3}$), dense ($n > 0.05\,\mathrm{cm}^{-3}$), hot diffuse ($T > 2\times10^5$ K, $n < 0.05\,\mathrm{cm}^{-3}$) and stripped ($Z > 0.01\,Z_\odot$, $n < 0.05\,\mathrm{cm}^{-3}$). Indeed, at $z = 3$ and 5 the mass accretion rates in cold streams is very high ($\dot{M} \simeq 20\,M_\odot\mathrm{yr}^{-1}$), however a significant amount of baryons are also accreted from stripped satellites. After $z \sim 2$ the hot mode of accretion dominates, making large clump formation at large radii only possible through galaxy mergers, c.f. E93 and Barnes & Hernquist (1992). At $z \sim 2$, the galaxy has a thin and extended spiral disk. Although the gas velocity dispersion is still rather high in the disk, the Jeans mass in the spiral arms is on the order of $\sim 10^7\,M_\odot$, closer to the largest GMCs in present day spiral galaxies. The corresponding gas Q_g-parameter (Goldreich & Lynden-Bell 1965) is $Q_\mathrm{g} \simeq 1.5-2$ in the star forming region, indicating that the disk is marginally stable and the galaxy has reached a quiescent phase with no further large clump formation.

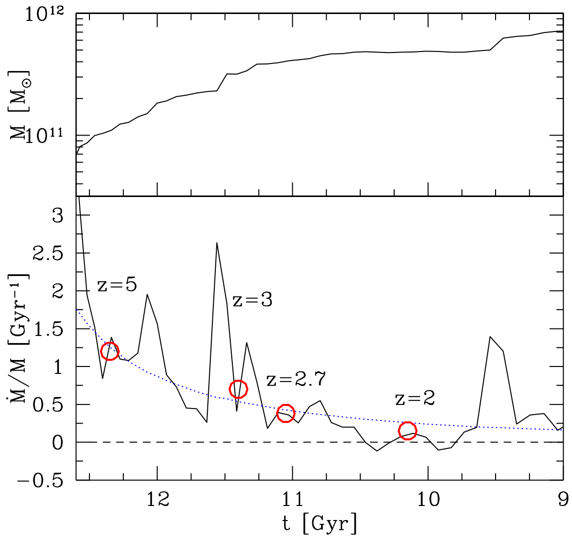

Figure 5. (*Top*) Dark matter accretion history for the VL-2 halo using the HOP halo finder. (*Bottom*) Logarithmic derivative of accretion history. After a period of moderate mass increase, during several epochs (e.g. $z \sim 3.25$ and ~ 1.75) the halo mass and hence the gaseous mass dramatically increases. The red rings mark specific times discussed in the text. The dotted blue line shows the expected averaged gas accretion calculated from EPS theory.

Fig. 5, shows the dark matter mass accretion rate in the simulated galaxy, as a function of time, together with the average mass accretion rate expected for a ΛCDM cosmology, as computed by Neistein et al. (2006). At $z = 2$, the accretion rate is significantly lower than the average, explaining why the disk has reached this quiescent phase.

4 CONCLUSIONS

We have followed the formation and accretion history of a Milky Way sized galaxy using high resolution AMR techniques. Our mass and spatial resolution is higher than that of any previous simulation including SPH techniques. Most of the baryons are in an orderly rotating disk by a redshift $z = 2$, but how they attain this equilibrium is very complex and the focus of this work. One of the most important points of this paper is that we can answer the question in detail of 'how galaxies get their baryons'. No single previous model is correct or complete - its not a cooling flow, its not a cold flow shocking at the disk radius, its mainly single phase narrow fragmenting cold streams and ram pressure stripped debris that directly forms a rotating disk due to the viscous rotational pressure of the inner hot halo.

Prior to $z > 2$, the accretion rate of cold gaseous material onto the disk is the highest and we resolve the formation of many very massive clumps within an extended ~ 10 kpc disk. This is several times larger than the theoretical expectations of disk sizes at this epoch (Mo et al. 1998). The observed morphology, star forming rate, global rotation and metallicity of the system is in good agreement with the observed clump-cluster and chain galaxies (Elmegreen & Elmegreen 2006; Elmegreen et al. 2007; Bournaud et al. 2008). This scenario is an extension of

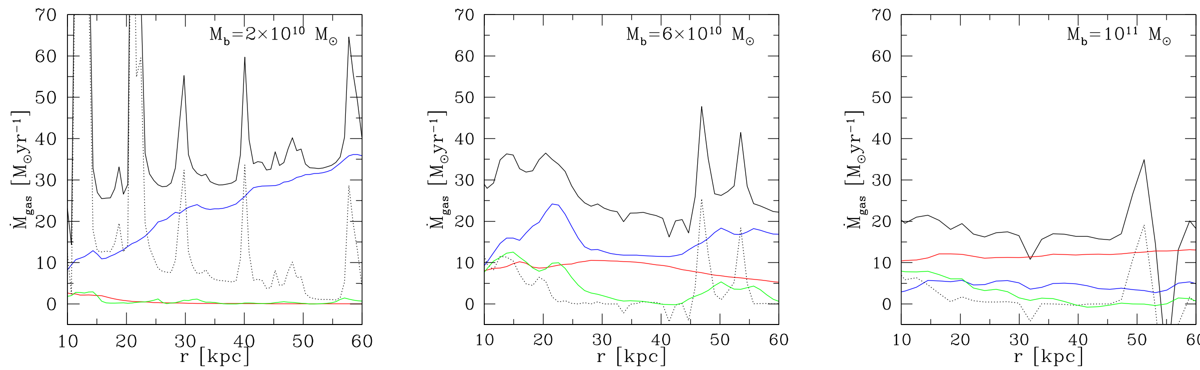

Figure 4. Mass accretion averaged within spherical shells at redshifts $z \sim 5, 3$ and 2. The radii are in physical kpc. The lines show the total mass flow (solid black) in each shell, cold diffuse (blue solid), hot diffuse (red solid), dense (dotted) and stripped gas (green) (see text for definition). We observe a decrease in the overall inflow of material and a change from cold to hot accretion over time.

the disk fragmentation scenario proposed by B07 and Elmegreen et al. (2008), although here studied more consistently within the current cosmological framework, and more specifically related to cosmological accretion. Therefore, clumpy galaxies should be most frequent at this epoch since massive clump formation stops during the remaining slow accretion phase and the disk evolves quiescently until $z = 0$, which will be reported on in a forthcoming paper.

ACKNOWLEDGMENTS

The authors would like to thank Aaron Boley for valuable discussion on gravitational instability. Thanks to Juerg Diemand for making the initial conditions available and to Doug Potter for making it possible to run the simulations on the zBox supercomputers (http://www.zbox2.org) at the University of Zürich.

REFERENCES

Agertz O., Lake G., Teyssier R., Moore B., Mayer L., Romeo A. B., 2009, MNRAS, 392, 294
Barnes J. E., Hernquist L., 1992, Nature, 360, 715
Birnboim Y., Dekel A., 2003, MNRAS, 345, 349
Bournaud F., Daddi E., Elmegreen B. G., Elmegreen D. M., Nesvadba N., Vanzella E., di Matteo P., Le Tiran L., Lehnert M., Elbaz D., 2008, A&A, 486, 741
Bournaud F., Duc P.-A., Emsellem E., 2008, MNRAS, 389, L8
Bournaud F., Elmegreen B. G., Elmegreen D. M., 2007, ApJ, 670, 237
Brooks A. M., Governato F., Quinn T., Brook C. B., Wadsley J., 2008, ArXiv e-prints
Cowie L. L., Hu E. M., Songaila A., 1995, AJ, 110, 1576
Daddi E., Cimatti A., Renzini A., Fontana A., Mignoli M., Pozzetti L., Tozzi P., Zamorani G., 2004, ApJ, 617, 746
Dalcanton J. J., Shectman S. A., 1996, ApJL, 465, L9+
Dekel A., Birnboim Y., 2006a, MNRAS, 368, 2
Dekel A., Birnboim Y., 2006b, MNRAS, 368, 2
Dekel A., Birnboim Y., Engel G., Freundlich J., Goerdt T., Mumcuoglu M., Neistein E., Pichon C., Teyssier R., Zinger E., 2008, ArXiv e-prints
Diemand J., Kuhlen M., Madau P., Zemp M., Moore B., Potter D., Stadel J., 2008, Nature, 454, 735
Dubois Y., Teyssier R., 2008, A&A, 477, 79
Elmegreen B. G., Bournaud F., Elmegreen D. M., 2008, ApJ, 688, 67
Elmegreen B. G., Elmegreen D. M., 2005, ApJ, 627, 632
Elmegreen B. G., Elmegreen D. M., 2006, ApJ, 650, 644
Elmegreen B. G., Elmegreen D. M., Ximena Fernandez M., Lemonias J. J., 2009, ApJ in press, 691
Elmegreen B. G., Kaufman M., Thomasson M., 1993, ApJ, 412, 90
Elmegreen D. M., Elmegreen B. G., Hirst A. C., 2004, ApJL, 604, L21
Elmegreen D. M., Elmegreen B. G., Ravindranath S., Coe D. A., 2007, ApJ, 658, 763
Förster Schreiber N. M. e. a., 2006, ApJ, 645, 1062
Genzel R. e. a., 2006, Nature, 442, 786
Genzel R. e. a., 2008, ApJ, 687, 59
Goldreich P., Lynden-Bell D., 1965, MNRAS, 130, 97
Jogee S. e. a., 2008, in Funes J. G., Corsini E. M., eds, ASPCS Vol. 396 of ASPCS, . pp 337–+
Keres D., Katz N., Fardal M., Dave R., Weinberg D. H., 2008, ArXiv e-prints
Kereš D., Katz N., Weinberg D. H., Davé R., 2005, MNRAS, 363, 2
Macciò A. V., Moore B., Stadel J., 2006, ApJL, 636, L25
Mo H. J., Mao S., White S. D. M., 1998, MNRAS, 295, 319
Neistein E., van den Bosch F. C., Dekel A., 2006, MNRAS, 372, 933
Ocvirk P., Pichon C., Teyssier R., 2008, MNRAS, 390, 1326
Overzier R. A., Heckman T. M., Kauffmann G., Seibert M., Rich R. M., Basu-Zych A., Lotz J., Aloisi A., Charlot S., Hoopes C., Martin D. C., Schiminovich D., Madore B., 2008, ApJ, 677, 37
Rasera Y., Teyssier R., 2006, A&A, 445, 1
Robertson B. E., Bullock J. S., 2008, ApJL, 685, L27
Romeo A. B., Agertz O., Moore B., Stadel J., 2008, ApJ, 686, 1
Shapiro K. L. e. a., 2008, ApJ, 682, 231
Tacconi L. J. e. a., 2008, ApJ, 680, 246
Taniguchi Y., Shioya Y., 2001, ApJ, 547, 146
Teyssier R., 2002, A&A, 385, 337
Truelove J. K., Klein R. I., McKee C. F., Holliman II J. H.,

Howell L. H., Greenough J. A., 1997, ApJL, 489, L179+
Wall J. V., Pope A., Scott D., 2008, MNRAS, 383, 435
Zheng W., Mikles V. J., Mainieri V., Hasinger G., Rosati P., Wolf C., Norman C., Szokoly G., Gilli R., Tozzi P., Wang J. X., Zirm A., Giacconi R., 2004, ApJS, 155, 73